NUMERICAL STUDY OF MELTING OF TIN WITHIN A RECTANGULAR CAVITY INCLUDING CONVECTIVE EFFECTS

Christiano Garcia da Silva Santim, chrisoff22@yahoo.com.br
Luiz Fernando Milanez, milanez@fem.unicamp.br
Universidade Estadual de Campinas, Caixa Postal: 6122 - 13083-970

Abstract. *This work deals with the numerical study of melting of pure tin within a rectangular cavity including the effects of convection. The cavity has one isothermally heated wall and the others are adiabatic. Initially the solid material is sub-cooled. The objective is to verify the influence of heating in the melting process, as well as sub-cooling effect. Several temperature profiles, streamlines and melting fronts were obtained for the system. Relations for the total melting time were derived as a function of the Stefan and Rayleigh numbers. Problems involving melting are nonlinear due to natural convection, which influences the melting front profile that varies with time. At the initial stages of the melting process, the heat transfer in the system occurs predominantly by heat conduction. The influence of natural convection on the melting process increases gradually with time and eventually it takes a dominant role. Some simplifying hypotheses were assumed in the mathematical model. The thermophysical properties of phase change material were considered constants, except for the density where the Boussinesq approximation was used. The problem was solved by using a mathematical formulation based on the enthalpy-porosity method, which allows the use of a fixed spatial grid. The liquid fraction is computed for each iteration, based on an enthalpy balance. The region where solid and liquid phases coexist is modeled as a "pseudo" porous medium, in which the porosity increases from 0 to 1 as the material liquefies. When the material is completely solidified in a cell the porosity becomes zero and thus also the velocities drop to zero. The computational grid used was selected after checking that the results did not vary with more refinement. The convergence criterion used for the energy equation was 10^{-8} while for the velocities and the continuity that criterion was lower, being 10^{-5} and 10^{-4} respectively.*

Keywords*: melting, phase change material, convective effects*

1. INTRODUCTION

Solidification and melting has great influences on nature and modern applications such as in metal purification and processing, in the latent heat thermal energy storage systems as well as in many other technologies. Problems involving phase change are non-linear due to natural convection. There are basically two methods to formulate phase change problems, one utilizes the temperature as a dependent variable in the energy equation, and the other utilizes the enthalpy.

The first experimental studies of melting inside rectangular geometries considering the convective effects were conducted by Hale and Viskanta (1978). The objective of their studies was to evidence the influence of natural convection in the melting process inside that geometry.

Okada (1984) analyzed numerically the melting process of n-octadecane paraffin from the heating of one of the vertical walls. The mathematical model was formulated in terms of the stream function and vorticity. Solutions were obtained for Rayleigh numbers greater than 5×10^6 and aspect ratio (width over height, in this case) up to 3. A transformation of coordinates was used so that the moving boundary (interface liquid-solid) could be immobilized. The results obtained in analytical form in this study, profile of the melting front and temperature distribution in the molten liquid region, were compared with experimental results obtained by the same author in Okada (1983). The author also presented a relation between the average Nusselt number along the heated vertical wall and the dimensionless time.

Gau and Viskanta (1986) conducted experiments regarding melting and solidification processes of gallium (purity of 99.6 %) with melting point at 29.78 ^{o}C, inside a rectangular recipient with one of the vertical walls heated. The authors proposed correlations between the volume of the molten metal and some dimensionless parameters. Temperature profiles were plotted, thus enabling a better analysis of the influence of natural convection in melting and solidification processes.

Brent *et al.* (1988) applied the mathematical formulation based on the enthalpy-porosity method in the melting of pure gallium, inside a rectangular cavity. The thermophysical properties of gallium were considered constants, except for the density, where the Boussinesq approximation was used. The rectangular cavity had an aspect ratio (height over width) of 0.714. The numerical results were compared with those obtained experimentally by Gau and Viskanta (1986) and showed good agreement, differently from what had happened with Webb and Viskanta (1986), that found similarity in the morphology of the liquid-solid interface, but a considerable discrepancy in its position. Therefore, the authors concluded that the formulation based on the enthalpy-porosity can be used satisfactorily in phase change problems.

Gong e Mujumdar (1998) studied the melting of a pure PCM in a rectangular container of aspect ratio of 0.5 heated from below (the top and the two vertical walls were assumed to be adiabatic) using the Streamline Upwind/Petrov Galerkin finite element method in combination with a fixed grid primitive variable method. The authors validated their

model comparing the results with those obtained by Gau and Viskanta (1986) and the implicit finite difference results of Lacroix (1992). The results presented showed that different flow patterns are obtained at different Rayleigh numbers. At high Rayleigh numbers, complex and time-dependent flow patterns were obtained.

Gong *et al*. (1999) analized numerically free convection-dominated melting of a PCM in a rectangular cavity with an isothermally heated vertical wall utilizing the same model employed by Gong e Mujumdar (1998). To enhance the heat transfer rate during the second half of the melting process, the authors proposed to invert the PCM container as the phase change interface reaches the right vertical wall of the container. The results obtained evidenced that the energy charge rate can be enhanced 52.4, 56.5 and 60.1 % in the second half of the melting process simply by inverting the PCM container for the cases of Rayleigh equal to 7.11×10^5, 2.844×10^6 and 5.688×10^6, respectively.

Le Quéré and Gobin (1999) presented a scale analysis of the parameters for wich flow instabilities can be expected in melting inside a rectangular cavity heated from the side. Prandtl values equals to 0.02 (gallium or tin) and 50 (octadecane) were employed. For each value of the Prandtl number, two values of the Rayleigh number were tested. The authors observed that for large nominal values of the Rayleigh number (aspect ratio greater than 10), multicellular instabilities are expected on the melting of pure low Prandtl number substances, strongly influencing the rate of heat transfer and the shape of liquid/solid interface. For high values of the Prandtl number cases the authors concluded that it is not clear wich type of instability could be obtained.

Hannoun *et al*. (2003) tried to clarify the controversy over tin and gallium melting inside a rectangular cavity heated from the side. Several issues were discussed about the influence of some parameters (grid sizes, discretization schemes, grid-converged solution) on the flow structure of melting process in this geometry. Previous experimental studies were discussed. In the numerical analysis, three commom discretization schemes (upwind, hybrid and centered) and several grid sizes were tested. The authors stated that the flow structure must be multicellular in melting inside a rectangular enclosure heated from the side.

Vidalain *et al*. (2009) presented a numerical model applicable to phase change problems based on the conduction equation for the solid and liquid phases. The model predicts the phase front position and the overall thermal behavior of the system without recurring to the full solution of Navier-Stokes equations. The effect of natural convection is taken into account by employing an enhanced thermal conductivity that depends on the geometry of the flow and the dimensionless numbers. The authors tested and confronted the model to full CFD solutions for a freezing duct flow problem and for buoyancy driven melting in an rectangular cavity and, in both cases, the predictions of the model proposed showed very good agreement with those of the CFD model.

In the present work, the melting of tin in a rectangular cavity is considered. The CFD Fluent code was used for the numerical simulation and the software Gambit was employed for the generation of the computational grid. The problem formulation was based on the enthalpy-porosity method, as suggested by Brent *et al.* (1988). The advantage of the utilization of this method is that, differently from the formulation based on the temperature, where the energy equation is applied separately for each phase, the conservation equations are valid for the whole domain (solid and liquid phase). Thus, as there is no need to determine explicitly the solid-liquid interface, the grid can be considered fixed.

The main objective of this work is to verify the influence of the isothermal heating of the left wall in the rectangular cavity, as well as the initial metal sub-cooling effect, in the melting process. Temperature and streamlines profiles were plotted to evidence the presence of natural convection during the process. Relations for the total melting time of tin as function of Rayleigh and Stefan dimensionless numbers were also obtained.

2. MATHEMATICAL FORMULATION

Three different temperatures (T_{hot}) were used in the isothermal heating of the rectangular cavity left wall: 510, 515 and 520 K. All other cavity walls were assumed adiabatic. At instant $t = 0$, all the phase change material are in the solid state, with uniform temperature. It should be noted that at this instant the solid is considered sub-cooled of 1 K. Such assumption was adopted for all the simulations, except when verifying the influence of the degree of the initial metal sub-cooling in the melting process, where sub-cooling of 1, 5 and 15 K were used, for a Stefan number of 0.022. The cavity aspect ratio was taken as 0.714. Simplifying hypotheses were taken in developing the mathematical model. The model was considered two-dimensional and transient. The flow in the melting process was assumed laminar and incompressible. The thermophysical properties of the material were considered constants. For the density, the Boussinesq approximation was used, where the density variation is considered only in the term relative to the buoyancy force in the Navier-Stokes equations. The physical model of the problem is presented in Fig. 1.

The numerical simulation was performed with the aid of a CFD Fluent code, utilizing the Solidification/Melting model, which employs a mathematical formulation based on the enthalpy-porosity. This formulation allows the use of a fixed spatial grid. The liquid fraction is computed at each iteration, based on an enthalpy balance. The region where solid and liquid phases of phase change material coexist is modeled as a "pseudo" porous medium, where the porosity increases from 0 to 1 as the material liquefies. When the material is completely solidified in a cell, the porosity becomes zero and consequently, the velocities also drop to zero. The enthalpy of the material, H, is computed as being the sum of the sensible enthalpy, h, and the latent heat, ΔH :

$$H = h + \Delta H \tag{1}$$

where ΔH is function of the temperature, and can be defined by:

$$f(T) = L \qquad T > T_m \tag{2}$$

$$f(T) = 0 \qquad T < T_m \tag{3}$$

In Eq. (2), L is defined as the latent heat of the material and T_m is the reference temperature.
The sensible enthalpy of Eq. (1), can be represented by

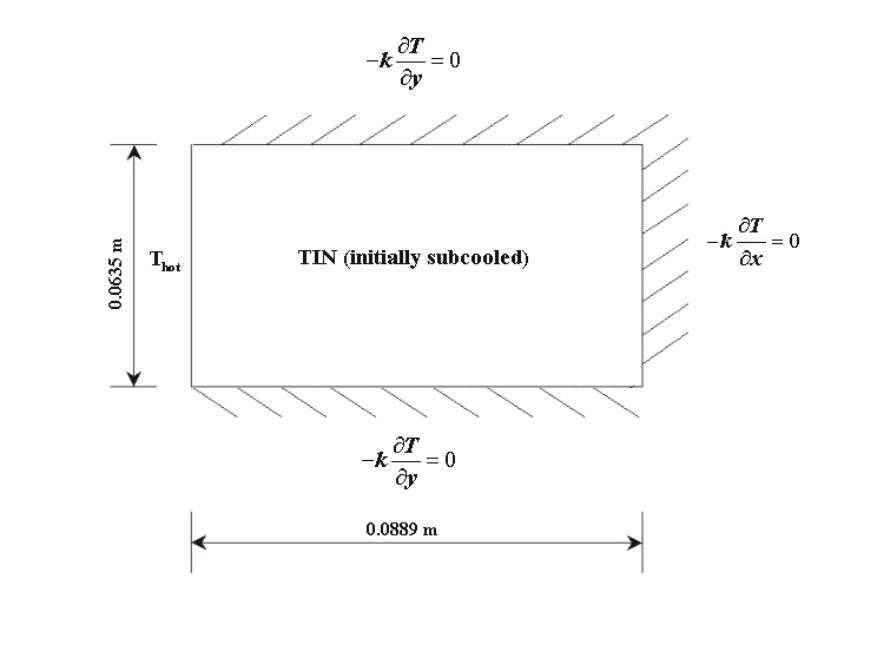

Figure 1. Physical model of the problem

$$h = h_m + \int_{T_m}^{T} c_p dT \tag{4}$$

where h_m is the reference enthalpy and c_p is the specific heat at constant pressure.
It should be stressed that the reference temperature (T_m) is considered in the present study as the tin melting temperature (505 K).
The energy conservation equation can be written as.

$$\frac{\partial(\rho H)}{\partial t} + \nabla.(\rho \boldsymbol{v} H) = \nabla.(k \nabla T) + S_e \tag{5}$$

where ρ is the density, $\boldsymbol{v}$ is a velocity vector ($\boldsymbol{v} = (u,v)$), k is the thermal conductivity and S_e is a source term.
The source term S_e can be calculated as

$$S_e = \frac{\partial(\rho \Delta H)}{\partial t} + \nabla.(\rho \boldsymbol{v} \Delta H) \tag{6}$$

In the regions where material in the liquid state is present, it is necessary to write equations for the flux. Assuming that the fluid is Newtonian and the flux is laminar, Eq. (7) is obtained for the mass conservation, Eq. (8) for the flux in the x direction, and Eq. (9) for the flux in the y direction, the last two equations representing the conservation of momentum (Navier-Stokes equations).

$$\frac{\partial \rho}{\partial t} + \nabla.(\rho \boldsymbol{v}) = 0 \tag{7}$$

$$\frac{\partial(\rho u)}{\partial t} + \nabla.(\rho \boldsymbol{v} u) = \nabla.(\mu \nabla u) - \frac{\partial P}{\partial x} + Su \tag{8}$$

where u is the velocity component in x direction, μ is dynamic viscosity, P is an effective pressure and S is the porosity function for the momentum equations.

$$\frac{\partial(\rho v)}{\partial t} + \nabla.(\rho \boldsymbol{v} v) = \nabla.(\mu \nabla v) - \frac{\partial P}{\partial y} + Sv + S_b \tag{9}$$

where v is the velocity component in y direction and S_b is the buoyancy source term.

The porosity function (S), present in Eq. (8) and Eq. (9), is defined as

$$S = -C\frac{(1-\gamma)^2}{\gamma^3 + \varepsilon} \tag{10}$$

where C is a constant reflecting the morphology of the melting front (this constant is a large number, usually 10^4 - 10^7), γ is the liquid fraction and ε is a small number (0.001) to prevent division by zero.

The S_b source term (Eq. (11)), in the v momentum equation (Eq. (9)), is a buoyancy term used to induce natural convection in the cavity (assuming the Boussinesq approximation).

$$S_b = \rho_m g \beta (T - T_m) \tag{11}$$

where β is a thermal expansion coefficient, ρ_m is the reference density and g is the acceleration of gravity.

The solver model utilized in the numerical simulation is the pressure-based. The coupling pressure-velocity is solved by the SIMPLE method. The scheme used in the discretization of momentum and energy conservation equations was the first order Upwind, and the scheme used for the pressure was the PRESTO!. The computational grid used was of 89 x 64 nodes in directions x and y, respectively, and it was selected after verification that the results were invariant with more refinement, that is, when the results were independent of the grid size. The convergence criterion for the energy equation was 10^{-8} and for the velocities and continuity was 10^{-5} and 10^{-4} respectively. The tin termophysical properties utilized in the computational simulation are presented in Tab. 1.

Table 1. Thermophysical properties of pure tin at 505 K

c_p (J/kg.K^{-1})	260
k (W/m.K^{-1})	46
ρ (kg/m^3)	7200
L (J/kg)	60000
μ (kg/m.s^{-1})	1.91x10^{-3}
β (1/K)	2.2x10^{-5}

3. RESULTS AND DISCUSSION

Brent *et al.* (1988) studied numerically the melting of gallium inside a rectangular cavity. Gau and Viskanta (1986) carried out the same study experimentally. Utilizing the same parameters assumed in the studies cited above, the results for the melting of gallium served to validate the scheme proposed in this work. Figure 2 shows the variation of the liquid fraction versus time for various Stefan number. The Stefan number (*Ste*) describes the operation condition of the cavity undergoing melting, given that the heated wall (T_{hot}) directly affects the value of the Stefan number and is defined as

$$Ste = \frac{c_p(T_{hot} - T_m)}{L} \tag{12}$$

The liquid fraction can be represented according to Eq. (13),

$$f = 1 - \frac{V_S}{V_C} \tag{13}$$

where f is the liquid fraction, V_S is the volume of solid and V_C is the volume of the rectangular cavity.

Analyzing Fig. 2 it may be noticed that the higher the Stefan number, the smaller is the time necessary for all the tin to be melted. With the rectangular cavity left wall heated at 510 K (*Ste* = 0.022), the total melting time of the metal was 4104 s, that is, it takes an additional 2287s to melt all the metal if the wall was heated at 515 K (*Ste* = 0.043), and 3004 s when compared with the wall heated at 520 K (*Ste* = 0.065). It may be noticed that the liquid fraction melted increases monotonically for all the cases considered.

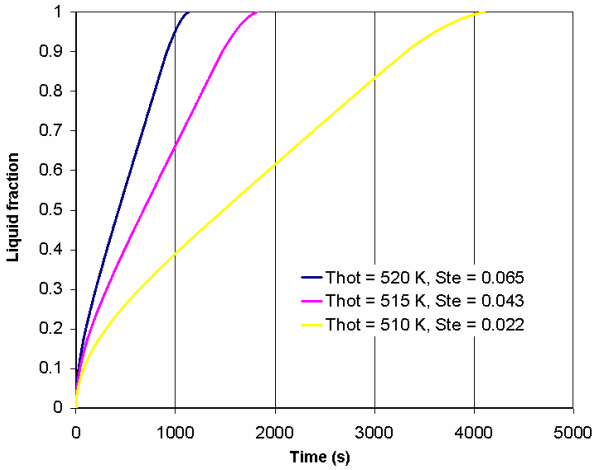

Figure 2. Liquid fraction for various Stefan number

Figure 3 shows the temperature distribution at y = 0.03175 m, for various times, for *Ste* = 0.065.

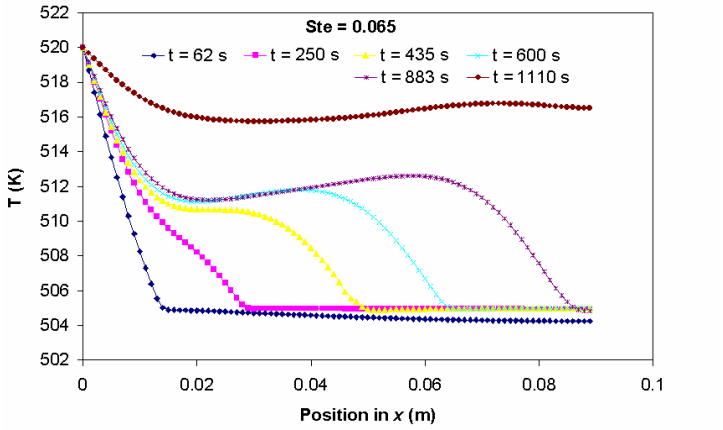

Figure 3. Temperature distribution along the center line (y = 0.03175 m) with T_{hot} = 520 K and sub-cooling of 1 K

It may be noticed in Fig. 3 that for t = 62 s the temperature distribution in the region of the melted liquid at y = 0.03175 m is practically linear. Such behavior is typical when conduction is the dominant heat transfer mechanism in the system. But as can be seen in Fig. 4 through the isotherms and streamlines, a convective flux begins to develop in the upper left region of the cavity at that instant. As the time increases, there is a gradual increase of the influence of natural convection in the melting process. The motion of the melted liquid, produced by buoyancy, results in a non-linear temperature distribution. In Fig. 3 this fact occurs for times higher than 62 s, when the convective flux begins in this region of the cavity.

Figure 5 shows flow and temperature fields at 250 s. It may be observed that the maximum value of the streamlines increased, showing that there is an intensification of the natural convection in the process. At that time, the influence of natural convection is more pronounced in the transport of energy, from the heated wall to the melting front. The melting front profile can be explained by the density difference of the melted liquid, where the higher temperature fluid tends to concentrate in the cavity upper region, and the colder fluid goes down. Such motion can be verified in Figs. 4 to 7 by the formation of a clockwise vortex.

Figure 6 shows that the melting process of tin, at t = 600 s, is mainly governed by natural convection. The maximum value of the stream function is 1.06. The temperature fields exhibit clearly the presence of the hotter fluid in the cavity upper region, causing the melting front of this region moves more quickly, compared to the lower region.

Figure 7 shows temperature and flow fields at 1110 s. Two vortices appear (besides the vortex already developed), one in each upper corner of the rectangular cavity, as can be observed in Fig. 7a. Such vortices exhibit a counter clockwise behavior but the central vortex is clockwise. When the tin is completely melted, the values of the streamlines tend to drop together with the temperature gradient.

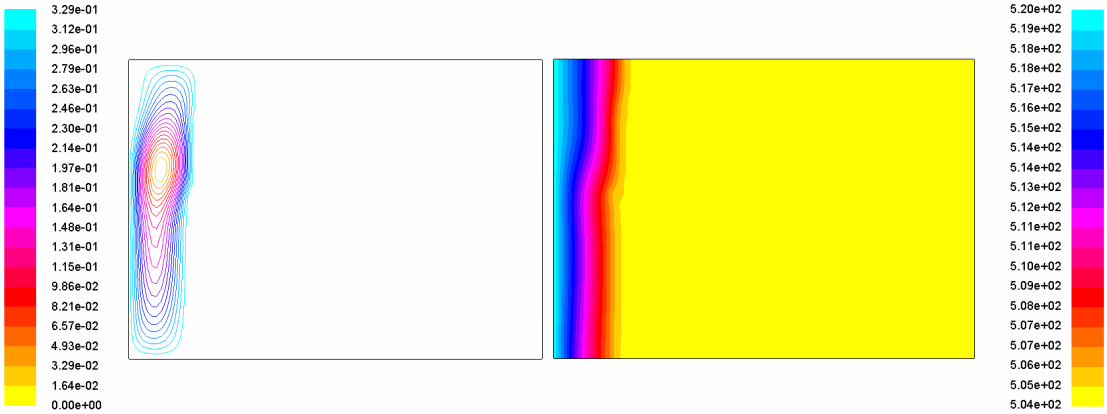

(a) (b)

Figure 4. Streamlines and temperature fields at 62 s for *Ste* = 0.065. (a) Streamlines; (b) Isotherms

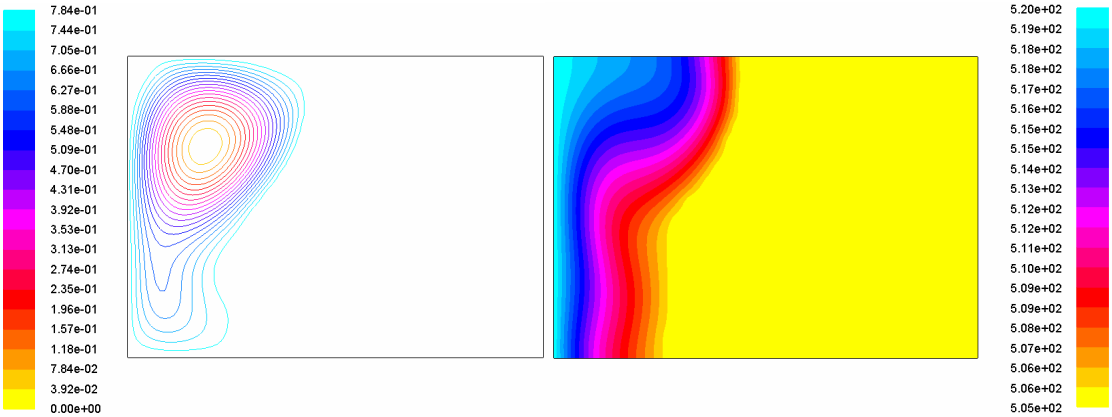

(a) (b)

Figure 5. Streamlines and temperature fields at 250 s for *Ste* = 0.065. (a) Streamlines; (b) Isotherms

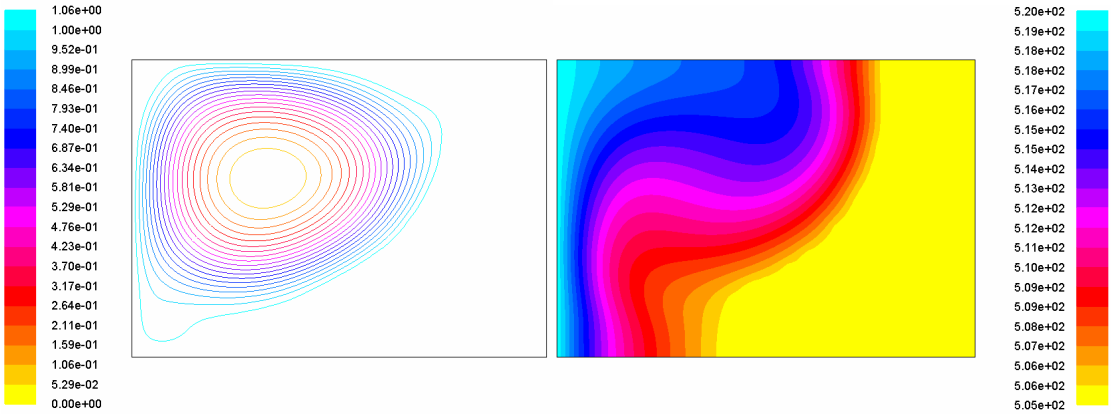

(a) (b)

Figure 6. Streamlines and temperature fields at 600 s for *Ste* = 0.065. (a) Streamlines; (b) Isotherms

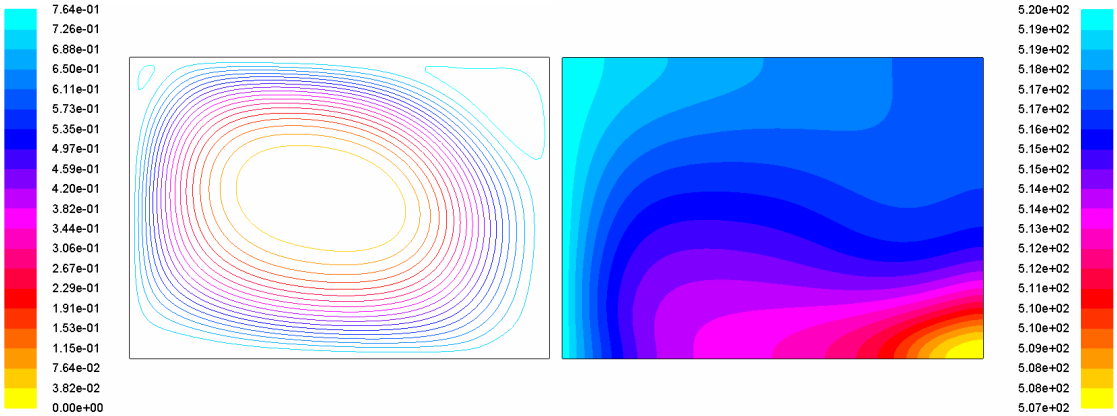

(a) (b)

Figure 7. Streamlines and temperature fields at 1110 s for *Ste* = 0.065. (a) Streamlines; (b) Isotherms

Figure 8 shows some positions of the tin melting front for three different values of the de Stefan number.

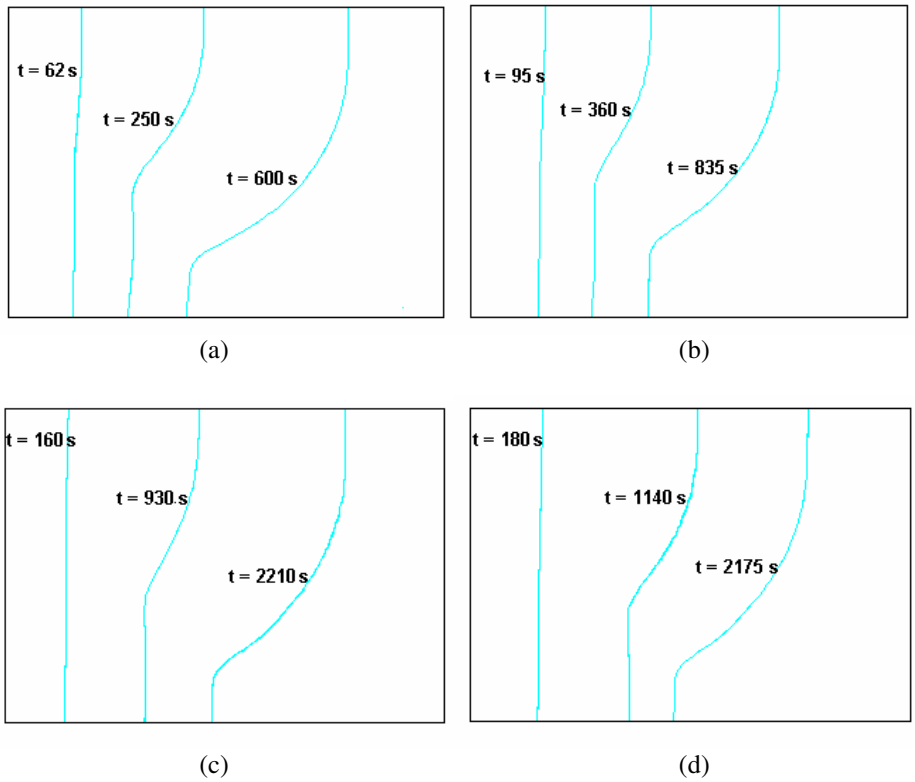

(a) (b)

(c) (d)

Figure 8. Comparison of melting front positions for various Stefan number. (a) *Ste* = 0.065, sub-cooling of 1 K; (b) *Ste* = 0.043, sub-cooling of 1 K; (c) *Ste* = 0.022, sub-cooling of 5 K; (d) *Ste* = 0.022, sub-cooling of 1 K

It may be noticed in Fig. 8 that the higher the value of the de Stefan number, the faster will be the movement of the melting front. The melting front profiles show the influence of the natural convection in the melting process. At the initial stages of the melting process the influence of the natural convection is not very strong because at this stage conduction is the dominant heat transfer mechanism. As the process develops, the upper region of the melting fronts moves faster than the lower region, evidencing a higher influence of the natural convection. The sub-cooling effect can be seen in Fig. 11. Such effect cannot be observed in Figs. 8c and 8d, because the melting front positions weren´t plotted for the same instants of time.

Figure 9 shows the time for complete melting of tin in terms of Rayleigh number (*Ra*). The Rayleigh number is defined as

$$Ra = \frac{g\beta(T_{hot} - T_m)y^3\rho}{\mu\alpha} \tag{14}$$

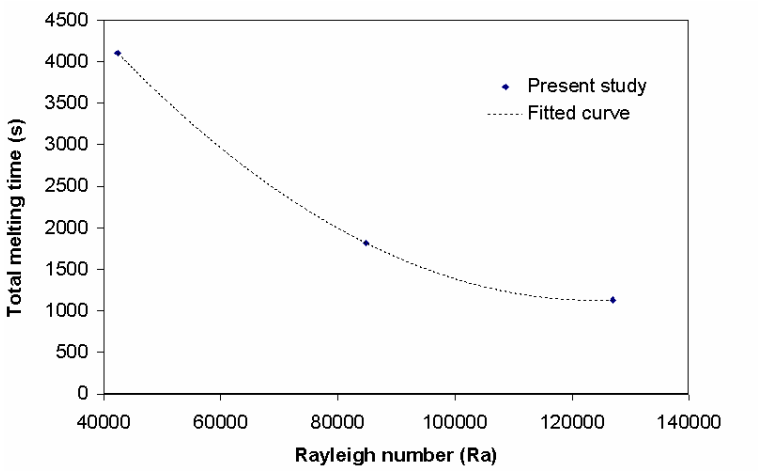

Figure 9. Total melting time in terms of the Rayleigh number

Observing Fig. 9 for values of the Rayleigh number higher than 1.2 x 10^5, the time for complete melting of tin drops at a rate well below than for values of Ra < 1.2 x 10^5. This behavior can be attributed to the fact that as the Rayleigh number is increased, the natural convection in the system is intensified and, therefore, a higher stabilization in the melting rate is reached.

Figure 10 shows the time for complete melting of tin in terms of Stefan number. The effect of the Stefan number in the melting process is very similar to the effect of the Rayleigh number.

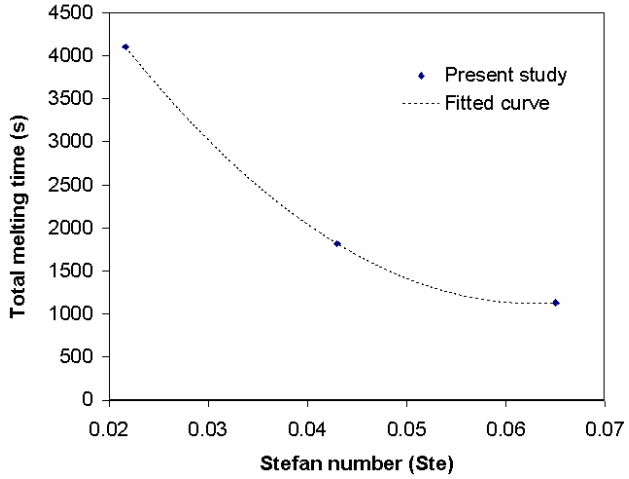

Figure 10. Total melting time in terms of Stefan number

The correlations relating the time for complete melting of tin to Stefan and Rayleigh numbers are presented below, Eq. (15) and Eq. (16) respectively, in the ranges $0.022 \leq Ste \leq 0.065$ and 4.24 x $10^4 \leq Ra \leq$ 1.27 x 10^5.

$$\tau_{fusão} = 1774740.7631(Ste)^2 - 224262.9115(Ste) + 8178.8095 \tag{15}$$

$$\tau_{fusão} = 4.3674 \text{ x } 10^{-7}(Ra)^2 - 0.10949(Ra) + 7961.3054 \tag{16}$$

where $\tau_{fusão}$ is the total melting time.

Figure 11 shows the variation of the liquid fraction for three different sub-cooling under melting for Ste = 0.022 (T_{hot} = 510 K).

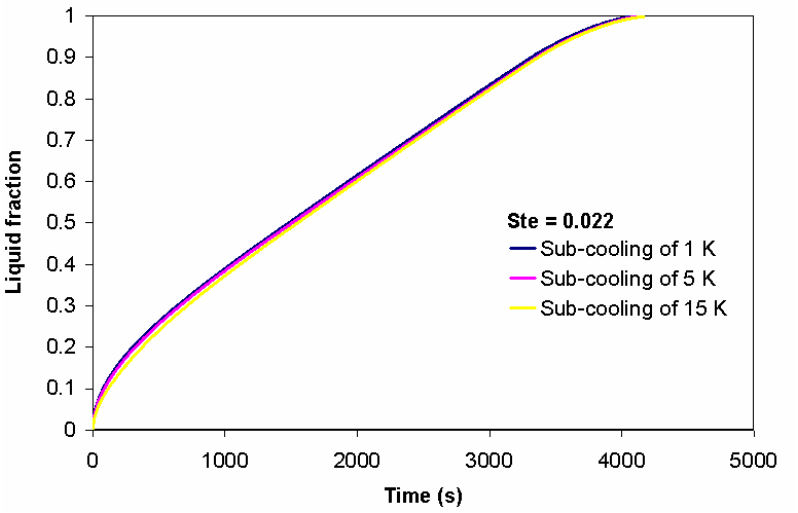

Figure 11. Effect of sub-cooling on the melting of tin

From Fig. 11 it may be noticed that when the solid is initially sub-cooled at 15 K, the total time for the complete melting, in this case being 4190 s, is almost the same when the sub-cooling is at 5 K (4144 s) or when the sub-cooling is at 1 K (4104 s). The fraction of the melted liquid exhibits almost the same behavior during the development of the process independently of the degree of sub-cooling, that is, the melting rates of the three curves are very similar. Therefore, the initial sub-cooling does not influence significantly the tin melting process.

4. CONCLUSIONS

In this study the melting process of tin inside a rectangular cavity, with one of the vertical walls isothermally heated was analyzed. From the results numerically obtained it was observed that in the initial stages of the melting process, the dominant heat transfer mechanism is conduction. The profiles of the streamlines, isotherms and melting fronts stressed the importance of the influence of natural convection during the process. Multicellular instability did not occur. The streamlines showed a unicellular flow during the process that was responsible for the melting front aspect and distribuition of themperatures in the liquid fraction. A multicellular flow was verified only when the material was fully melted. Therefore, multicells had no influence in the rate of melting and morphology of melting front in this case. Correlations for the total tin melting time as a function of the dimensionless numbers of Stefan and Rayleigh were presented.

Utilizing three different degrees of sub-cooling for the same Stefan number, it was observed that the fact that the material is initially sub-cooled does not affect significantly the tin melting process, and the total melting times were very close. The melting rates during the process were also almost the same.

5. ACKNOWLEDGEMENTS

The authors wish to thank the CAPES for financial support.

6. REFERENCES

Brent, D., Voller, V.R. and Reid, K.J., 1988, “Enthalpy-Porosity Technique for Modeling Convection Diffusion Phase Change: Application to the Melting of a Pure Metal”, Numerical Heat Transfer, Vol.13, pp. 297-318.

Gau, C. and Viskanta, R., 1986, “Melting and Solidification of a Pure Metal on a Vertical Wall”, Journal of Heat Transfer, Vol.108, pp. 174-181.

Gong, Z.-X., Devahastin, S. and Mujumdar, A.S., 1999, “Enhanced Heat Transfer in Free Convection-Dominated Melting in a Rectangular Cavity with an Isothermal Vertical Wall”, Applied Thermal Engineering, Vol.19, pp. 1237-1251.

Gong, Z.-X. and Mujumdar, A.S., 1998, “Flow and Heat Transfer in Convection-Dominated Melting in a Rectangular Cavity Heated from Below”, International Journal of Heat and Mass Transfer, Vol.41, pp. 2573-2580.

Hale Jr., N.W and Viskanta, R., 1978, “Photographic Observation of the Solid-Liquid Interface Motion During Melting of a Solid Heated from an Isothermal Vertical Wall”, Lett. Heat Mass Transfer, Vol.5, pp. 329-337.

Hannoun, N., Alexiades, V. and Mai, T.Z., 2003, “Resolving the Controversy over Tin and Gallium Melting in a Rectangular Cavity Heated from the Side”, Numerical Heat Transfer, Part B, Vol.44, pp. 253-276.

Lacroix, M., 1992, " Predictions of Natural Convection-Dominated Phase Change Problems by the Vorticity–Velocity formulation of the Navier–Stokes Equations", Numerical Heat Transfer, Part B, Vol.22, pp. 79–93.

Le Quéré, P. and Gobin, D., 1999, "A Note on Possible Flow Instabilities in Melting from the Side", Int. J. Therm. Sci., Vol.38, pp. 595-600.

Okada, M., 1983, "Melting from a Vertical Plate Between Insulated Top and Bottom Surfaces", Proc. ASME/JSME Thermal Engng. Joint. Conf., Vol.1, pp. 281-288.

Okada, M., 1984, "Analysis of Heat Transfer During Melting from a Vertical Wall", International Journal of Heat and Mass Transfer, Vol.27, pp. 2057-2066.

Vidalain, G., Gosselin, L. and Lacroix, M., 2009, "An Enhanced Thermal Conduction Model for the Prediction of Convection Dominated Solid-Liquid Phase Change, Vol.52, pp. 1753-1760.

7. RESPONSIBILITY NOTICE

The authors are the only responsible for the printed material included in this paper.